

# Analysis of Physico-Chemical Processes in an Amperometric Oxygen Biosensor

S. Krishnamoorthy, J. J. Feng and V. B. Makhijani  
CFD Research Corporation, 215 Wynn Drive  
Huntsville, AL 35806, USA, [sk@cfdr.com](mailto:sk@cfdr.com)

Chuan Gao, Jin-Woo Choi and Chong H. Ahn  
Dept. of Electrical & Computer Engineering and Computer Science  
University of Cincinnati, Cincinnati, OH

## ABSTRACT

Amperometric techniques are commonly used in lab-on-a-chip systems to sense various blood gas analytes such as H<sup>+</sup>, CO<sub>2</sub>, O<sub>2</sub>, etc. In the present study, a microchip-based amperometric biosensor, being developed as a part of plastic-based structurally programmable microfluidic chip for clinical diagnostics at University of Cincinnati, is analyzed. For accurate modeling of electrokinetic transport and detection of various electroactive species, two levels of modeling are coupled: (i) fluid flow and transport of analytes and (ii) electrochemical surface reactions. In the present work, we have coupled the electrokinetic transport module [1][2] with electrochemical surface reaction solver. A detailed analysis of the system at the diffusion limit reveals that although the temperature variations are insignificant, the measured signal varies significantly due to Joule heating. An interesting phenomenon of increased sensitivity due to electrode-edge effect, caused by singularity at electrode edges, is also observed and discussed.

**Keywords:** Amperometric Biosensor, microfluidics, CFD-ACE+, modeling, lab-on-a-chip

## 1 INTRODUCTION

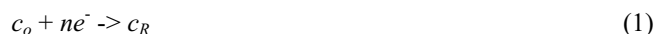
Electrochemical transduction methods are very popular in sensing biological components. The performance and utility of a sensor lie in its ability to discriminate between different substrates (selectivity), to produce signals for sub-millimolar up to femtomolar concentration (sensitivity), and to reproduce signals within reasonable margin of error (accuracy) [4]. Besides the response time (time to produce stable signal) and recovery time (time before it is ready to analyze next sample) are expected to be shorter. Microchip implementation of sensors enables compact size, integrated functions of sample separation and detection (lab-on-a-chip), low cost due to batch production and potential parallel analysis. Consequently, design, fabrication and commercialization of these systems require understanding the fundamental physical mechanisms associated with electrokinetic transport of various analytes, fluid flow and electrochemical reactions at the sensor surface. In this

regard, numerical analysis can provide insight into the interactions between various physical processes so that systems' performance can be improved and/or optimized.

Electrochemical biosensors use electrochemical methods for transduction. They can be subdivided in to three types [4]: (a) Potentiometric sensors that involve the measurement of potential of a cell at zero current (the potential proportional to logarithm of the concentration of the substrate being measured); (b) Amperometric sensors where an oxidizing (or reducing) potential is applied between cell electrodes and the cell current is measured. (the height of the peak current in the diffusion limit proportional to the concentration of the electroactive species); and (c) Conductimetric sensors that use the relationship between the conductance and ionic species' concentration to measure the concentration of the substrate. In the present work, an amperometric biosensor developed at University of Cincinnati to measure oxygen concentration in blood sample is used in the analysis. It is a component of a plastic-based structurally programmable lab-on-a-chip system and is being developed at Professor Ahn's laboratory. The modeling effort is an extension of our work presented at MSM2000 [1] and MSM2001 [2].

## 2 MATHEMATICAL MODELING

In amperometric biosensors, the electrode reaction produces a measurable current that is a measure of the rate of the electrochemical reaction and is proportional to the concentration of the electro-active species. The reaction may be expressed as:



where  $c_o$  is the oxidizable specie,  $e^-$  is an electron,  $n$  is number of electrons transferred during the reaction and  $c_R$  is the reducible species. The increasing rate of reduction causes the cell current to increase. The net current in system is given by the algebraic sum of cathodic and anodic currents:

$$i = nFk^0 \left[ c_o \exp \left[ -\frac{\alpha nF(\phi - \phi^0)}{RT} \right] - c_R \exp \left[ -\frac{(\alpha - 1)nF(\phi - \phi^0)}{RT} \right] \right] \quad (2)$$

where  $n$  is the valence of the electroactive specie,  $F$  is Faraday constant,  $k^0$  is the kinetic constant,  $c_o$  is the concentration of oxidized specie,  $c_R$  is the concentration of reduced specie,  $\alpha$  is the symmetric coefficient,  $\phi$  is the applied voltage,  $\phi^0$  is the reference voltage,  $R$  is the universal gas constant and  $T$  is the absolute temperature. The overall current is limited by the fact that the concentration of  $c_o$  is rapidly depleted by the surface reaction and the current is limited by the rate of diffusion of fresh  $c_o$  from the bulk solution. The value of the diffusion-limited current is obtained from the Fick's first law of diffusion as:

$$i = nFD \frac{dc_o}{dn} \quad (3)$$

where  $D$  is the diffusion coefficient and  $n$  denotes normal to the cathode surface. In diffusion limit, the current density is not sensitive to the over-potential and give rises to the maximum measurable value.

The generalized transport equation for ionic species is expressed as:

$$\frac{\partial c}{\partial t} + \nabla \cdot (n\mu Ec - D\nabla c) = 0 \quad (4)$$

where  $n$  is the valence of the ion,  $\mu$  is the mobility,  $E$  is the electric field vector,  $c$  is the molar concentration of the analyte, and  $D$  is the diffusion coefficient. To compute the electric field  $E$ , we need to solve the continuity equation for current

$$\nabla \cdot j = 0 \quad (5)$$

where  $j$  is the flux that can be described by generalized Ohm's law.

### 3 PROBLEM DESCRIPTION

The coupled nonlinear partial differential equations (1), (3) to (5) were solved using CFD Research Corporation's advanced multi-physics commercial software package, CFD-ACE+. The implicit finite-volume technique discussed in [3] is used to solve the governing equations. The schematic of the biosensor analyzed is shown in Figure 1.

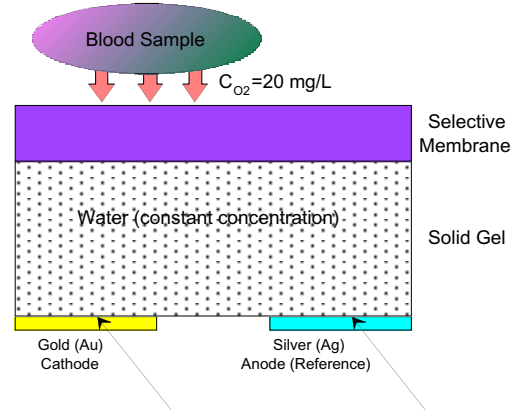


Figure 1: Schematic of Biosensor Developed at University of Cincinnati

The biosensor consists of a gel sandwiched between a selective membrane and electrode. The solid gel liquefies at high temperature and provides sufficient amount of water for the surface reaction at the cathode. Anode reaction only supplies electrons needed in cathode reaction. The sample is kept at the top of the membrane. The reduction of oxygen occurs at the cathode and the signal is measured externally. For the modeling purpose, transport through selective membrane was ignored as a first approximation. The gel is considered as a porous media and the diffusion coefficient of oxygen is modified as per porosity of the medium. A constant voltage is applied at the cathode and the current is calculated as a part of the solution.

### 4 RESULTS AND DISCUSSIONS

Various electrode designs used in the study are summarized in Figure 2. All designs have same anodic and cathodic area, while the edge length of cathode in Design D and E is twice that of Design A.

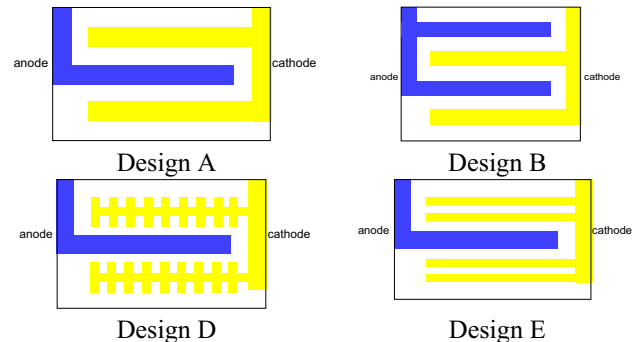


Figure 2: Different Electrode Designs Studied

Effect of Electrode Area: The experiments were performed at University of Cincinnati and the steady state or peak current was measured for various electrode areas (the width of the electrodes were changed, while the distance between anode and cathode was kept constant). The results from the

simulation are shown in Figure 3 and compared with experimental data.

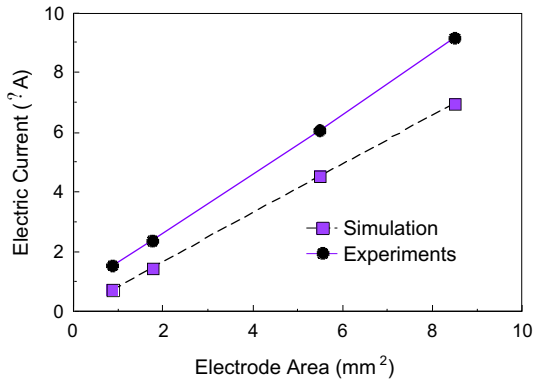


Figure 3: Comparison of Experimental Data and CFD-ACE+ Simulation Data.

There is about 25% difference between experiments and modeling, although the linearity of the current with respect to the electrode area is observed in both cases. The discrepancy between CFD-ACE+ and experimental data may be attributed to neglecting oxygen transport through the selective membrane, reconstitution of the electrolyte and subsequent changes in the diffusivity of the oxygen. Theoretical investigation of these phenomena is currently underway.

Effect of Sample Concentration: In Figure 4, oxygen concentration in the sample is varied and the signal was measured. As expected, ACE+ results predicted linear variation in signal with respect to oxygen concentration since the sensor was operated at its peak current.

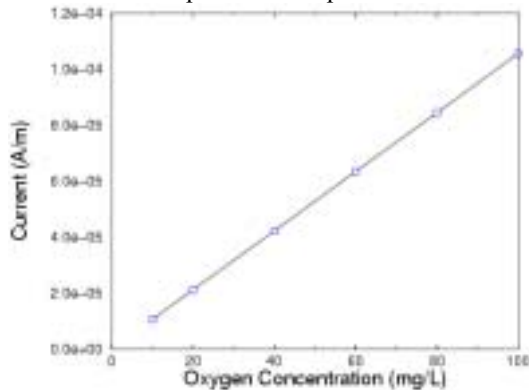


Figure 4: Predicted Peak Current As a Function of Oxygen Concentration in the Blood Sample

Effect of Electrolyte Thickness: In Figure 5, we have simulated performance of oxygen sensor by varying both electrolyte thickness (10 to 50  $\mu\text{m}$ ) and sample concentration (10 to 100 mg/L). Oxygen diffusion is largely one-dimensional above the cathode. This leads to an inverse linear relationship between current density and the total thickness of sensor.

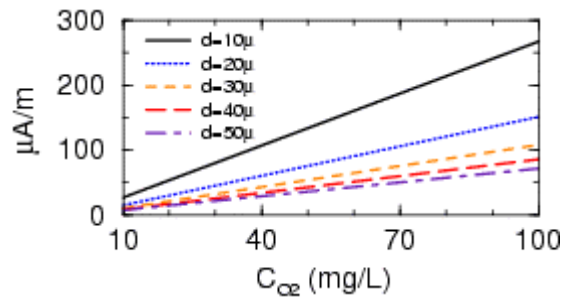


Figure 5: Current Density as a Function of Oxygen Concentration and Gel Thickness

Effect of Joule Heating: In the experiments, there may be two sources for heat generation: heating from the bottom of the sensor and Joule heating within the sensor. Joule heating arises from local electric current that generates heat source inside the gel. The source term due to Joule heating is expressed as:

$$(6)$$

where  $E$  is the externally imposed electric field and  $\sigma$  is the electrical conductivity of the medium. We use Stokes-Einstein relation to approximate diffusivity as a function of temperature as:

$$(7)$$

Results from 2D simulation are shown in Figure 6. Here the electrolyte thickness of 30  $\mu\text{m}$  is used. As expected, the electric field is very high in the region between two electrodes. This figure suggests that the overall temperature increases by 0.1% due to Joule heating and it can be neglected. However, as shown in Figure 7, the increase in the diffusivity of oxygen, leading to an increase in current density by as much as 6%, cannot be neglected. Besides, with heating, the current equilibrates slightly faster.

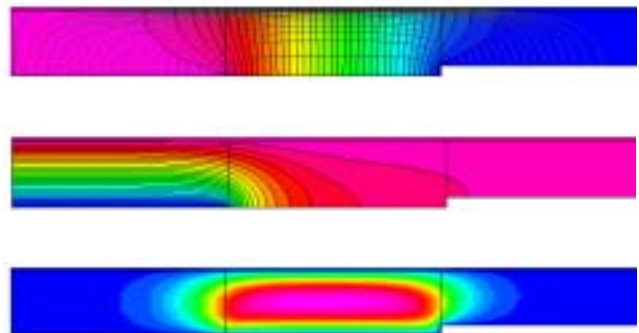


Figure 6. Simulation results from 2D simulation for electrolyte thickness of 30 $\mu\text{m}$ , Design B at steady state. (a) Contour plot of Electric potential and Electric field line. (b) Oxygen concentration distribution. (c) Temperature field due to Joule heating alone.

## 5 CONCLUSIONS

In this work a computational model has been developed for predicting the peak current in an amperometric oxygen sensor. The model solves for transport of electroactive species coupled with the electrochemical reaction and potential distribution in a tightly coupled manner. The simulations show that increasing the electrode area and/or minimizing the gel thickness is critical in increasing the sensitivity and detection time. The signal can be further improved by simply changing the geometry of the electrodes. For example, the simulation predicts that the change in the edge length of the electrode while keeping the same area can increase the sensitivity by as much as 12%. Experimental verification of this edge effect is currently underway at University of Cincinnati. Besides, increasing the electrode area also increases the peak current, however, the size and shape of the electrode may be limited by manufacturing process and overall system dimension. A designer cannot ignore the Joule heating while developing a sensor. For the case discussed in this paper, an increase in temperature by 0.1% increased the peak current by 6%, when operated at the diffusion limit. The present study clearly shows that a MEMS designer has the opportunity to implement variety of design modification while designing a biosensor. In this aspect, simulation tools will help in the optimization of biosensor based on the trade-off between compactness and performance.

### Acknowledgement

The authors wish to acknowledge the financial support from DARPA/MTO SIMBIOSYS program. The authors like to thank Dr. Z. J. Chen for useful discussions and Ms. Misty Gravette for preparing this manuscript.

## 6 REFERENCES

- [1] S. Krishnamoorthy and M.G. Giridharan, "Analysis of Sample Injection and Band-Broadening in Capillary Electrophoresis Microchips", *Proceedings of 2000 International Conference on Modeling and Simulation of Microsystems*, pp. 528-531, San Diego, CA, 2000.
- [2] S. Krishnamoorthy, J. J. Feng and V. B. Makhijani, "Analysis of Sample Transport in Capillary Electrophoresis Microchip using Full-Scale Numerical Analysis", *Proceedings of 2001 International Conference on Modeling and Simulation of Microsystems*, Hilton Head, SC, 2001.
- [3] CFD-ACE+, Version 6.6, *Users Manual*, CFD Research Corporation, Huntsville, AL, USA, 2001.
- [4] B. Eggins, *Biosensors, An Introduction*, John Wiley & Sons, New York, NY, 1997.

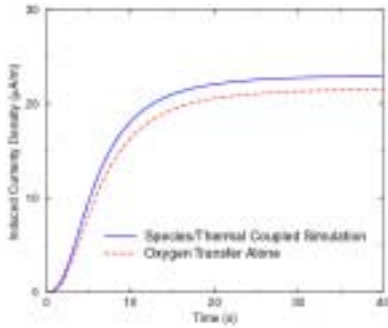


Figure 7. Influence of Joule Heating on Induced Current Density

**Effect of Electrode Edge Length:** In this section we investigate, the effect of edge length on the peak current. Two electrode designs, D and E (Figure 2), were investigated. Both design have the same area, however have twice the edge length as that of baseline Design A. Results from the numerical simulation are shown in Figure 8 where the induced current density is compared.

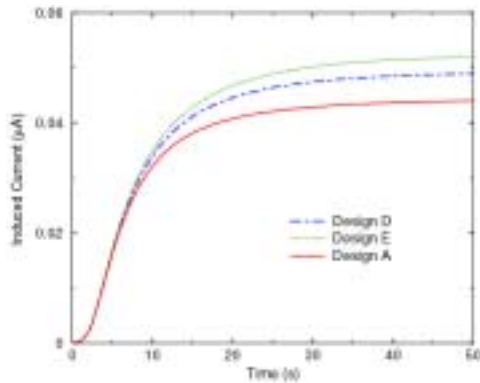


Figure 8. Comparison of induced current between Designs D, E and A

It is observed that there is an increase in induced current density by 8% for Design D and 12% for Design E. The surface concentration oxygen for these two configurations is shown in Figure 9. Detailed inspection indicates that the increase of current was due to pile up (large gradient) of the oxygen ions across the edges of the cathode

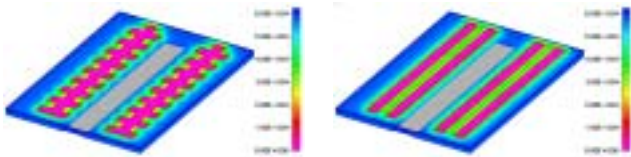


Figure 9. Concentration contour of Oxygen near the cathode for designs D and E.